Orientational Order of a Liquid Crystal with Three Chiral Centers by a Combined ^{13}C NMR and DFT Approach

R. Y. Dong,*,†,‡ M. Geppi,§ A. Marini,§,|| V. Hamplova,⊥ M. Kaspar,⊥ C. A. Veracini,§ and J. Zhang‡

Department of Physics and Astronomy, University of British Columbia, 6224 Agricultural Road, Vancouver, British Columbia, Canada V6T 1Z1, Department of Physics and Astronomy, University of Manitoba, Winnipeg, Manitoba, Canada R3T 2N2, Dipartimento di Chimica e Chimica Industriale, Università di Pisa, v. Risorgimento 35, 56126 Pisa, Italy, Scuola Normale Superiore, Piazza dei Cavalieri 7, 56126 Pisa, Italy, and Institute of Physics, Academy of Sciences of the Czech Republic, Na Slovance 2, 182 21 Prague, Czech Republic

Received: April 20, 2007; In Final Form: June 15, 2007

In this work, the liquid crystal (*S*)-2-methylbutyl-[4′-(4″-heptyloxyphenyl)-benzoyl-4-oxy-(*S*)-2-((*S*)-2′)-benzoyl)-propionyl)]-propionate (ZLL 7/*) was investigated by means of ^{13}C NMR spectroscopy. This compound has a very peculiar mesomorphic behavior, showing the following phases: paraelectric SmA, ferroelectric SmC*, antiferroelectric SmC*$_A$, re-entrant ferroelectric SmC*$_{re}$, and ferroelectric hexatic Sm*$_{HEX}$. The structural and orientational ordering properties of ZLL 7/* have been determined by exploiting the nuclear chemical shielding properties of ^{13}C. To this aim, solid-state NMR techniques such as CP, SPINAL-64, and SUPER have been used in combination with DFT calculations. The agreement between experimental and in vacuo DFT shielding parameters appears to be satisfactory. The orientational order parameters obtained from the ^{13}C shielding analysis have been discussed, taking into account different data analysis approaches and comparing them to those previously obtained from an independent ^{2}H NMR study.

1. Introduction

^{13}C NMR is a powerful method for investigating orientational order, magnetic shielding properties, and molecular motions in liquid crystals (LC)[1] and, in particular, in chiral smectic phases.[2] In anisotropic media, the chemical shift interaction is described for each carbon site by a chemical shift tensor (δ), defined in an arbitrary coordinate system. This produces a characteristic powder pattern in non-rotating solids, with a peak at the principal element δ_{yy}, the middle value in the diagonalized δ tensor, and sharp steps at the two other principal components. Such powder patterns due to chemical shift anisotropy (CSA) have the advantage of giving the magnitudes of the principal components of the δ tensor directly either with or without spectral simulations. A recent 2-D method for rotating solids, termed the separation of undistorted powder patterns by effortless recoupling (SUPER), was proposed[3] to obtain CSA powder patterns using suitably rotation-synchronized radio frequency (r.f.) pulses. SUPER was shown to be an easy and more reliable technique with respect to the existing techniques aimed to determine CSA principal values, such as 2-D TOSS-deTOSS,[4] MAT,[5] etc. It has already produced a number of ^{13}C powder spectra in organic solids and polymers for different chemical sites (aromatic, unprotonated sp^2-hybridized, and aliphatic). More recently, it has also been applied successfully on bent-core LC molecules in the solid state.[6,7] Besides representing a valid aid in the spectral assignment of the ^{13}C spectra of mesogens, the CSA principal values experimentally obtained by SUPER can be exploited in the determination of orientational order parameters in the LC phases, as obtained from the chemical shift values measured from ^{13}C static spectra. However, this would require knowledge of the orientation of the diagonalized δ tensor with respect to the molecular frame where the orientational ordering Saupe matrix is defined. To this aim, ab initio methods, giving the complete nine-element shielding matrix for each ^{13}C nucleus, can be helpful. Recent achievements in density functional theory (DFT) calculations have made possible a satisfactorily accurate evaluation of the δ tensor components for several molecular systems.[8] Thus, the comparison between theoretical and experimental CSA principal values represents an important step in the perspective of obtaining reliable orientational ordering properties from ^{13}C NMR spectra.

In the present paper, the SUPER method was employed in the solid phase of the chiral mesogen (*S*)-2-methylbutyl-[4′-(4″-heptyloxyphenyl)-benzoyl-4-oxy-(*S*)-2-((*S*)-2′)-benzoyl)-propionyl)]-propionate (ZLL 7/*) at ambient temperature, and the experimental CSA principal values have been compared with those obtained from in vacuo DFT calculations. The results so obtained have been used to obtain orientational order parameters from the ^{13}C chemical shift values, determined for all of the carbon nuclei of the rigid molecular core using static ^{13}C spectra recorded in several LC phases of ZLL 7/*. In particular, efficient decoupling schemes available nowadays, such as SPINAL-64,[9] are exploited to achieve the required good spectral resolution.

This paper is organized as follows: section 2 includes all of the experimental details of sample preparation and NMR and DFT calculation methods; section 3 contains the SUPER experimental results and their comparison with those obtained

* Corresponding author. Tel.: (604) 822-3898. Fax: (604) 822-5324. E-mail: rondong@phys.ubc.ca.
† University of British Columbia.
‡ University of Manitoba.
§ Università di Pisa.
|| Scuola Normale Superiore.
⊥ Academy of Sciences of the Czech Republic.

10.1021/jp0730693 CCC: $37.00
Published on Web 07/27/2007

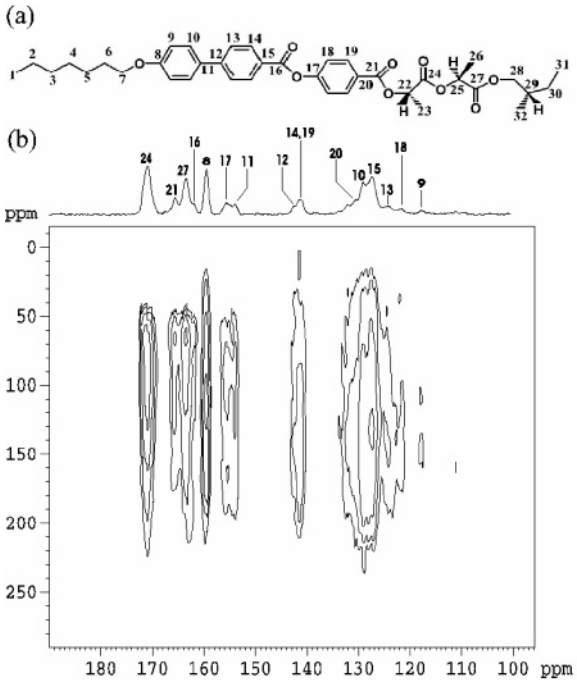

Figure 1. (a) Chemical structure of ZLL 7/* with carbon site labels, (b) typical SUPER 2-D spectrum taken at room temperature (only the aromatic region is emphasized). Top trace represents the 1-D proton-decoupled ^{13}C spectrum.

by DFT methods; section IV describes experimental ^{13}C anisotropic chemical shifts; and section V contains the analysis of orientational order from ^{13}C anisotropic chemical shifts. This is followed by a brief summary.

2. Experimental Procedures

2.1. Sample and Mesomorphic Behavior. The chiral liquid crystal ZLL 7/* shows various mesophases at different ranges of temperature. Its structure is sketched in Figure 1a. The transition temperatures of ZLL 7/* were reported before as follows:[10]

$$\text{iso} \xleftrightarrow{129\,^\circ\text{C}} \text{SmA} \xleftrightarrow{104\,^\circ\text{C}} \text{SmC*} \xleftrightarrow{98\,^\circ\text{C}} \text{SmC}^*_\text{A} \xleftrightarrow{71\,^\circ\text{C}}$$
$$\text{SmC}^*_\text{re} \xleftrightarrow{65\,^\circ\text{C}} \text{Sm*}_\text{HEX} \xleftrightarrow{54\,^\circ\text{C}} \text{crystal}$$

The synthesis of the ZLL 7/* compound and its basic properties have previously been published.[11]

2.2. SUPER Experiment. The 2-D ^{13}C SUPER experiment was carried out at 100.6 MHz on a solid ZLL 7/* sample rotating at a spinning speed (f_{rot}) of 4.8 kHz at room temperature using a Bruker Avance 400 solid-state system with a 4 mm double resonance CP-MAS probe. The sample temperature was regulated to within 0.1° by means of air flow. Without sample rotation, the CSA produced characteristic powder patterns with a peak at δ_{yy} and sharp steps at the two other principal values. Under MAS, such CSA powder patterns could be observed in the first dimension of a 2-D MAS experiment provided that suitably rotor-synchronized r.f. pulses were implemented. The SUPER experiment, which correlates CSA powder patterns in the f_1 dimension with the isotropic chemical shifts in the f_2 dimension, is based on the experiment of Tycko et al.[12] but can provide a better compensation for experimental imperfections such as inhomogeneous r.f. (B_1) fields. The scaling factor of CSA (set at 0.155) is also more favorable. Its pulse sequence is shown in Figure 2a.[3] After a 90° (4.2 μs) proton irradiation

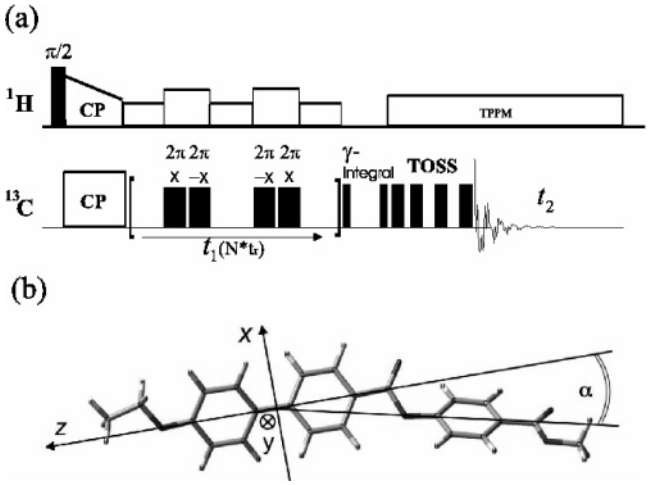

Figure 2. (a) Schematic of SUPER pulse sequence. Intervals of the z-filters during the γ integral are given by $t_z = kt_r/4$ ($k = 1,...,4$). (b) Molecular model used to perform DFT calculations on ZLL 7/*.

and a ramp cross-polarization (CP) of 2 ms, four ^{13}C 2π pulses were used to recouple CSA during MAS. The ^{13}C r.f. power level required for recoupling was $f_{r.f.} = 12.12f_{rot}$. To avoid the signal being dephased by strong heteronuclear couplings during the recoupling 2π pulses, a continuous wave (cw) proton decoupling field of 69 kHz was applied. The spinning sidebands were removed by TOSS in combination with the γ integral.[13] The γ integral contains an increment of the z-filter period in four steps of $t_r/4$. During acquisition, the TPPM15[14] decoupling sequence was applied at a decoupling level of 30 kHz. The number of t_1 increments was 32. The STATES-TPPI[15] quadrature detection and a recycling time of 3 s were used.

2.3. ^{13}C NMR Spectra. Solution-state spectra were recorded, at room temperature, on a Varian Unity 300 spectrometer, operating at 75.42 MHz for ^{13}C and at 299.93 MHz for ^{1}H, by dissolving the samples in $CDCl_3$. ^{13}C NMR experiments on the neat ZLL 7/* were carried out on a double-channel Varian Infinity Plus 400 spectrometer, working at 100.56 MHz for ^{13}C, equipped with either a 5 mm goniometric probe or a 7.5 mm CP-MAS probe. Static spectra were recorded from the NMR glass tube filled with the sample in the goniometric probe. For MAS experiments, the sample was put in a glass ampule, sealed by epoxy glue, to fit in the ZrO_2 rotor. MAS spectra were recorded with a spinning frequency of 6.0 kHz. To obtain well-resolved ^{13}C$-^1$H NMR spectra in the whole mesomorphic range, both static and MAS experiments were carried out under high-powered ^{1}H-decoupling conditions by means of the SPINAL-64 technique[9] at a decoupling field of about 44 kHz. SPINAL-64 has become the method of choice to perform proton decoupling in LC because of its better performance in spectral resolution. The ^{1}H$-^{13}$C CP technique with a linear ramp on the carbon channel was used in all of the cases, using a contact time of 7 and 10 ms for static and MAS experiments, respectively, accumulating 400−4000 scans, and using a relaxation delay of 4 s to minimize r.f. heating effects due to ^{1}H decoupling. The ^{1}H 90° pulse length was always 4.3 μs. The temperature was controlled to within 0.2 K. A temperature calibration was performed for the applied experimental conditions by exploiting the known phase transition temperatures of some LC. The sample was macroscopically aligned within the superconducting magnet by slow cooling from the isotropic phase before collecting the ^{13}C spectra in the LC phases. On cooling, a 30 min temperature stabilization period was taken at each temperature before acquiring the spectrum. Different

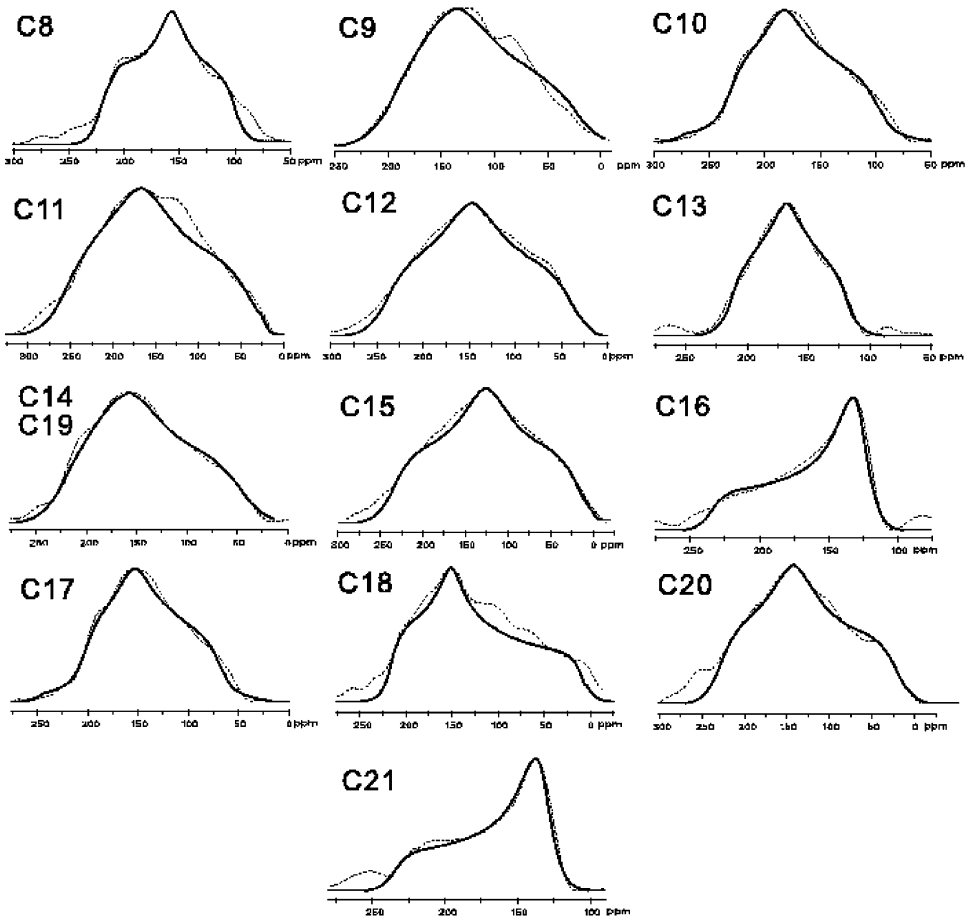

Figure 3. CSA powder patterns obtained from f_1 dimension of Figure 1b.

cooling rates and temperature equilibration times were applied to check the reproducibility of the different phase transition temperatures.

2.4. DFT Methods. Methyl-[4′-(4″-ethyloxyphenyl)-benzoyl-4-oxy]-benzoate, represented in Figure 2b, was used as a model for the mesogen ZLL 7/*, and it was built by GaussView 3.0.[16] All the calculations were performed by Gaussian 03[16] using in vacuo DFT methods. Geometries and carbon nuclear shielding tensors were determined, for the different conformers of the model compound having high statistical weights, at the DFT level of theory using B3LYP/6-31G(d) and MPW1PW91/6-311+G(d,p)[17] in combination with hybrid functional and basis sets, respectively. NMR chemical shielding tensors were calculated by the method of Gauge-Including Atomic Orbitals, GIAO.[18] The chemical shift tensors were obtained by referring the absolute chemical shielding tensors obtained by DFT to the absolute shielding of TMS (185.97 ppm), which was calculated at the same level of theory as the ZLL 7/* model. The value of σ_{iso} for TMS obtained by GIAO-DFT calculations is very close to that (185.4 ppm) obtained after correction by vibrational averaging, bulk susceptibility, temperature, and relation to a secondary standard.[19] This result confirms the appropriateness of the basis set and functional used in the GIAO-DFT calculations.

3. SUPER Experimental Results and Chemical Shift Tensor DFT Calculations

Figure 1b shows a typical 2-D SUPER spectrum (only the aromatic carbonyl region is emphasized) in the solid phase of ZLL 7/*, together with the 1-D isotropic spectrum (f_2 projection) showing ^{13}C peak assignments given at the top. The CSA powder patterns of different carbon sites can be retrieved from the f_1 slices of Figure 1b as shown in Figure 3. The assignment of the aromatic carbon signals is based on the isotropic chemical shift prediction using commercial software, the comparison with solution-state spectra, and the observed CSA powder patterns. Each observed powder line shape (dotted lines) was simulated using the WSOLIDS simulation package[20] to determine the principal components of the CSA tensor, and the simulations are shown as solid curves in Figure 3 for direct comparison.

The principal components of the chemical shielding tensor, so obtained for each inequivalent ^{13}C nucleus in the rigid core of ZLL 7/*, are reported in Table 1, together with the corresponding principal values calculated via DFT methods. From a careful analysis of each δ tensor, one can distinguish between different topological situations experienced by different ^{13}C nuclei belonging to the same functional group (i.e., tertiary and quaternary aromatic carbons, carbonyl carbons). In particular, it is possible to observe that the quaternary carbons C8 and C17, connected to an electron-donating group (OR), are easily distinguishable from the other quaternary aromatic carbons because they have very large out-of-plane δ_{yy} components.[21] On the contrary, the quaternary carbons C15 and C20, connected to an electron-withdrawing group (COOR), exhibit the smallest δ_{yy} components.[22] The carbonyl carbons C16 and C21 have chemical shift tensors characterized by $\delta_{xx} \approx \delta_{yy} \ll \delta_{zz}$.[21] C9, being in the β position with respect to the alkoxy group, experiences both the lowest δ_{zz} and the lowest δ_{yy}.[22] With all these facts considered, the values obtained for the principal components of each δ tensor are in very good agreement with those reported in the literature for similar compounds.[4,5,23]

TABLE 1: Comparison of δ Principal Values for Aromatic and Carbonyl Carbon Sites of ZLL 7/* as Obtained by SUPER and DFT (Latter Are in Parentheses)[a]

sites	C8	C9	C10	C11	C12
δ_{yy}	99.2 (100.0)	23.0 (22.9)	27.6 (25.7)	38.8 (36.9)	39.7 (40.4)
δ_{xx}	156.7 (158.2)	134.0 (130.1)	135.6 (139.9)	166.8 (171.0)	147.7 (151.2)
δ_{zz}	222.7 (220.3)	195.0 (199.2)	223.6 (221.9)	255.8 (253.4)	239.7 (235.3)
θ	0.0 (0.0)	60.0 (59.5)	120.0 (119.6)	180.0 (180.0)	0.0 (0.0)
sites	C13	C14	C15	C16	C17
δ_{yy}	45.0 (37.1)	45.2 (42.5)	18.0 (18.8)	122.7 (122.0)	77.0 (72.0)
δ_{xx}	132.0 (134.3)	157.2 (160.5)	127.0 (129.2)	128.7 (125.3)	154.0 (152.8)
δ_{zz}	195.0 (200.6)	221.2 (220.0)	236.0 (233.1	234.7 (237.2)	237.0 (238.2)
θ	60.0 (60.9)	120.0 (120.8)	180.0 (180.0)	120.0 (124.5)	0.0 (0.0)

sites	C18	C19	C20	C21
δ_{yy}	24.3 (17.3)	45.2 (45.8)	20.5 (25.4)	128.0 (127.6)
δ_{xx}	147.3 (140.1)	157.2 (157.9)	142.5 (140.1)	135.0 (136.5)
δ_{zz}	213.3 (206.0)	221.2 (218.1)	228.5 (225.8)	234.5 (232.4)
θ	60.0 (59.2)	120.0 (119.5)	180.0 (180.0)	120.0 (116.2)

[a] θ is angle between the *z*-axis of the chemical shift principal axes frame and the para-axis of the relevant aromatic fragment; values obtained assuming "regular" geometry and derived from DFT calculations (in parentheses) are reported.

The agreement between theoretical and experimental chemical shift principal values (see Table 1) is quite satisfactory (the average deviation is about 3 ppm), particularly if we consider that these data originate from two different structural situations: the 2-D SUPER experiments were carried out in the solid phase, while the DFT calculations were performed in vacuo. The surrounding medium can induce either structural modifications (indirect effect) or, for a given structure, electron density distribution modifications (direct effect). In this work, these effects have not been taken into account: this is probably the main source of deviation between calculated and experimental shielding tensors.

4. ^{13}C Anisotropic Chemical Shifts

For each carbon nucleus in the molecule, the chemical shift measured from static ^{1}H-decoupled ^{13}C spectra ($\delta_{\mathbf{obs}}$) in the uniaxial LC phases is related to orientational order parameters and chemical shift tensor elements (δ_{ab}) by the following equation:

$$\delta_{\mathbf{obs}} = \delta_{\mathbf{iso}} + \frac{2}{3}\Big[\Delta\delta \mathbf{S}_{zz} + \frac{1}{2}(\delta_{xx} - \delta_{yy})(\mathbf{S}_{xx} - \mathbf{S}_{yy}) + 2\delta_{xy}\mathbf{S}_{xy} + 2\delta_{xz}\mathbf{S}_{xz} + 2\delta_{yz}\mathbf{S}_{yz}\Big] \quad (1)$$

where

$$\Delta\delta = \delta_{zz} - \frac{1}{2}(\delta_{xx} + \delta_{yy}) \quad (2)$$

is the anisotropy of δ with respect to the molecular *z*-axis, the Saupe ordering matrix **S** is defined in a molecular (*x*,*y*,*z*) frame, and the tensor δ is written in the same frame. $\delta_{\mathbf{iso}}$ is the isotropic chemical shift (i.e., one-third of the trace of the chemical shift tensor): to correctly take into account possible conformational and/or phase packing effects, this must be taken temperature by temperature from the corresponding ^{13}C MAS spectra, rather than from ^{13}C spectra in solution or in the solid state. The tensor δ written in the molecular frame can be related to that defined in its principal axes system (PAS) by means of the following equation:

$$\delta_{ab} = \sum_{\epsilon} \cos\theta_{\epsilon a} \cos\theta_{\epsilon b}\delta_{\epsilon\epsilon} \quad (3)$$

where $\theta_{\epsilon a}$ is the angle between the ϵ principal axis and the *a* molecular axis.

Indeed, the main limitation in employing ^{13}C anisotropic chemical shifts measured from static ^{1}H-decoupled spectra arises from the need of knowing the shielding tensor in the molecular coordinate system where the orientational order Saupe matrix is defined. This problem can be overcome by a combined theoretical and experimental approach. The principal values of the shielding tensor can be determined by the SUPER technique, and these values can be used to validate the theoretical shielding tensor obtained by DFT calculations: if theoretical and experimental tensors agree, the DFT calculations can reliably give the relative orientation of the PAS frame of the shielding tensor with respect to the molecular frame where the Saupe matrix is defined, thus overcoming the assumption of regular geometry. In our case, the agreement between DFT and experimental principal values of the shielding tensors was very good, as was previously pointed out (see Table 1). Moreover, the orientational order parameters derived from this approach could be compared with those previously obtained by an independent ^{2}H NMR study.[10]

4.1. Assignment of ^{13}C Spectra. Before discussing the analysis of the anisotropic chemical shifts in terms of orientational order parameters, it must be noted that the assignment of the ^{13}C static spectra recorded in the mesophases was often a non-trivial task because of the combined dependence of the observed chemical shift from the chemical shielding tensor components (differing from carbon to carbon) and order parameters, which often renders some difficulties in the correlation between $\delta_{\mathbf{obs}}$ and the isotropic chemical shift values. The assignment of solution-state ^{13}C spectra (not shown) for ZLL 7/* has been carried out on the basis of ^{13}C DEPT, ^{1}H−^{13}C HETCOR, and ^{1}H spectra. The values of ^{13}C isotropic chemical shifts obtained from solution-state spectra are reported in Table 2, where they are compared with those either obtained from the MAS experiments recorded in the mesophases, or determined in the solid state (from the projection of the 2-D SUPER experiment), or determined by means of in vacuo DFT-GIAO calculations.

Considering that the different sets of data are for quite different structural situations (solution, mesophase, solid, isolated molecule), the agreement among them appears to be quite good (for most carbon nuclei, the maximum deviations are within 3−4 ppm). However, a few carbon nuclei (C11, C12, C14, and

TABLE 2: Isotropic Chemical Shifts δ_{iso} (in ppm) for Aromatic and Carbonyl Carbon Sites of ZLL 7/* as Obtained by Solution ^{13}C Spectra, ^{13}C CPMAS Spectra in Liquid−Crystalline Phases, Projection of SUPER Experiment Carried Out in Solid Phase, and in Vacuo DFT Calculations[a]

carbon no.	δ_{iso} solution	δ_{iso} MAS (mesophases)	δ_{iso} SUPER (solid)	δ_{iso} DFT (in vacuo)
8	159.91	160.8	159.5	159.5
9	115.23	116.0	117.7	117.4
10	128.62	128.5	129.1	128.9
11	146.49	145.5	153.8	153.8
12	133.02	145.5	142.3	142.3
13	126.89	126.6	124.1	124.0
14	135.04	131.8	141.2	141.0
15	129.21	128.5	127.0	127.0
16	164.73	165.6	162.0	161.5
17	155.30	156.0	155.6	154.3
18	122.10	122.9	121.6	121.1
19	134.81	131.8	141.2	140.6
20	127.18	126.6	130.5	130.4
21	165.42	165.6	165.6	165.5

[a] Reported CPMAS δ_{iso} values are an average over the whole mesophasic range; the trends of δ_{iso} vs temperature throughout the mesophasic range do show small variations (see Supporting Information). Carbon numbers refer to Figure 1a.

C19) exhibit larger deviations, suggesting that they might be more sensitive to conformational and/or molecular packing changes through the different phases. Nevertheless, even though the various signals have been attributed to the different carbon nuclei with care by exploiting all the information available from different experiments, theoretical predictions, and literature data, the uncertainties present in the assignment in a few cases were removed based on the criterion of minimizing the differences among the different sets of δ_{iso}.

A selection of the ^{13}C CP static spectra recorded in the different mesophases of ZLL 7/* is shown in Figure 4, while in Figure 5, the trends of δ_{obs} versus temperature for all of the distinguishable ^{13}C signals in the aromatic carbonyl region are reported. Thirteen different signals can be distinguished for 16 inequivalent carbons (12 aromatic and four carbonyl) of ZLL 7/*. The signals belonging to the aromatic tertiary carbon nuclei can be easily recognized on the basis of their characteristic δ_{obs} values, in the range of 135−165 ppm. Both aromatic and carbonyl quaternary carbons have instead chemical shifts between 185 and 230 ppm. To distinguish these two kinds of carbons, one can merely compare their typical δ_{obs} versus temperature trends, which in the case of carbonyl carbons show less variations.[23] Also, within the aromatic resonances, those belonging to the biphenyl moiety have been determined on the basis of their slightly less pronounced temperature dependence.[23] The assignment of the different quaternary and tertiary carbons within phenyl or biphenyl moieties has been carried out on the basis of different values of $\Delta\delta$ evaluated by DFT methods or determined by 2-D SUPER experiments. The assignment reported in Figure 5 has been validated a posteriori by verifying that this corresponded to the best agreement between experimental and calculated δ_{obs} values in their global analysis in terms of orientational order parameters.

4.2. Temperature Dependence of ^{13}C Chemical Shift. The various transition temperatures of ZLL 7/* can be easily detected from the trends of both δ_{obs} and linewidths of each ^{13}C signal with temperature. Within the SmA phase, δ_{obs} values for all of the aromatic and carbonyl carbons regularly increase with decreasing temperature due to the increase in the orientational order; the line width of each signal is very sharp (40−60 Hz). By entering the SmC* phase, all of the lines clearly broaden (linewidths of 250−300 Hz), and δ_{obs} assumes higher values than in the SmA phase, as is usually found when the helix described by the directors in the SmC* phase is unwound by the magnetic field.[24] By decreasing the temperature within the very small SmC* range, δ_{obs} decreases as a consequence of the transformation of the unwound into the wound SmC* phase.[25] This is in agreement with a previous ^{2}H NMR study (performed at the same magnetic field of 9.4 T employed here), where these two phases have been found to coexist throughout the SmC* range, the wound one becoming increasingly more populated upon decreasing temperature.[10] At the SmC*−SmC*$_A$ transition, it is possible to observe both a small jump down for δ_{obs} and a decrease in the line width (130−150 Hz) (see Figures 4 and 5). Within the SmC*$_A$ phase, δ_{obs} decreases, reaches a minimum, and then increases again for all of the ^{13}C signals, as a result of the combined effects of the orientational order and the tilt angle, both increasing by lowering the temperature, thus tending, respectively, to increase and decrease δ_{obs}. In the re-entrant SmC*$_{re}$ phase, the lines broaden again (linewidths of 350−430 Hz), and δ_{obs} rises up more steeply.

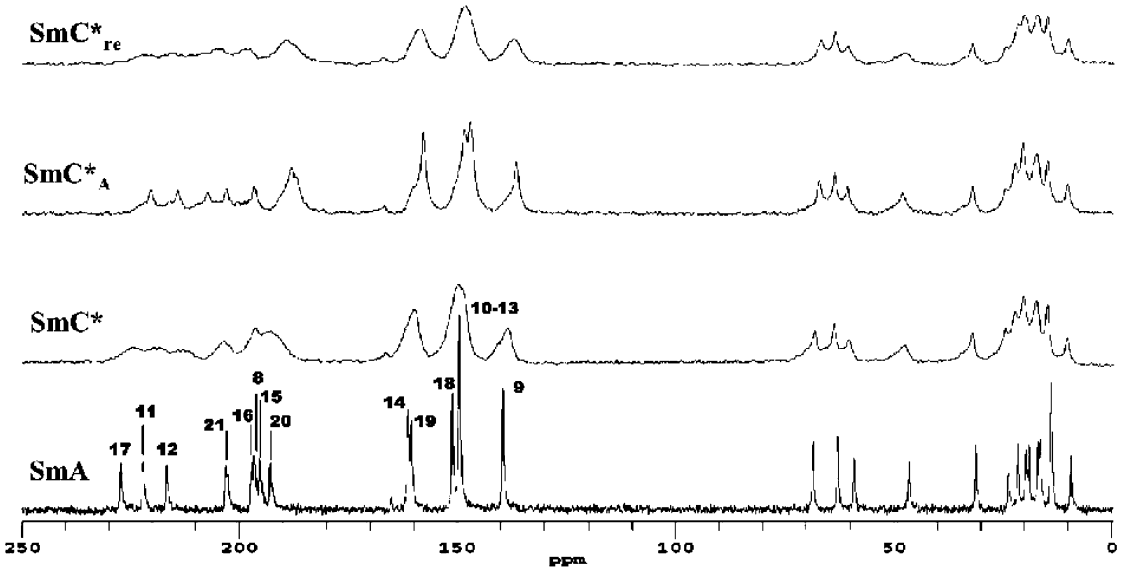

Figure 4. Selection of ^{13}C CP spectra recorded in various mesophases of ZLL 7/* under static conditions and SPINAL-64 ^{1}H-decoupling.

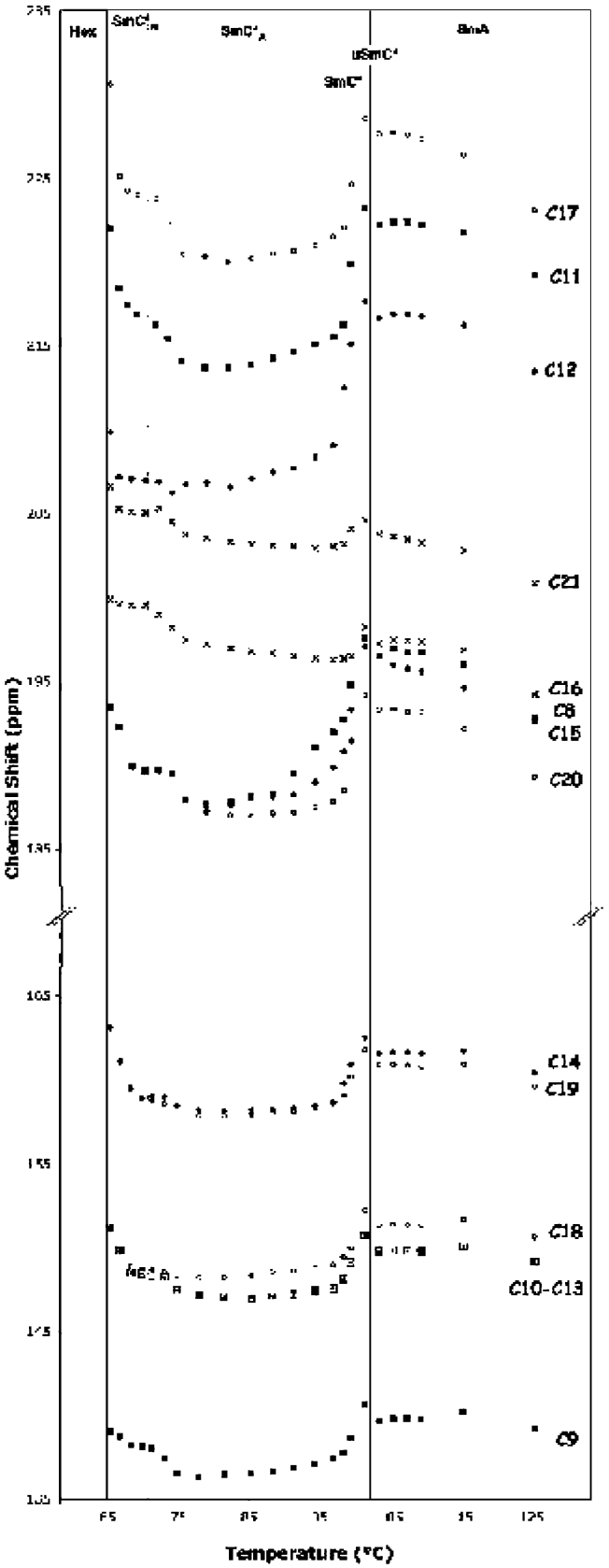

Figure 5. Plots of δ_{obs} vs temperature for different aromatic and carbonyl ^{13}C signals. Carbon labeling refers to Figure 1a.

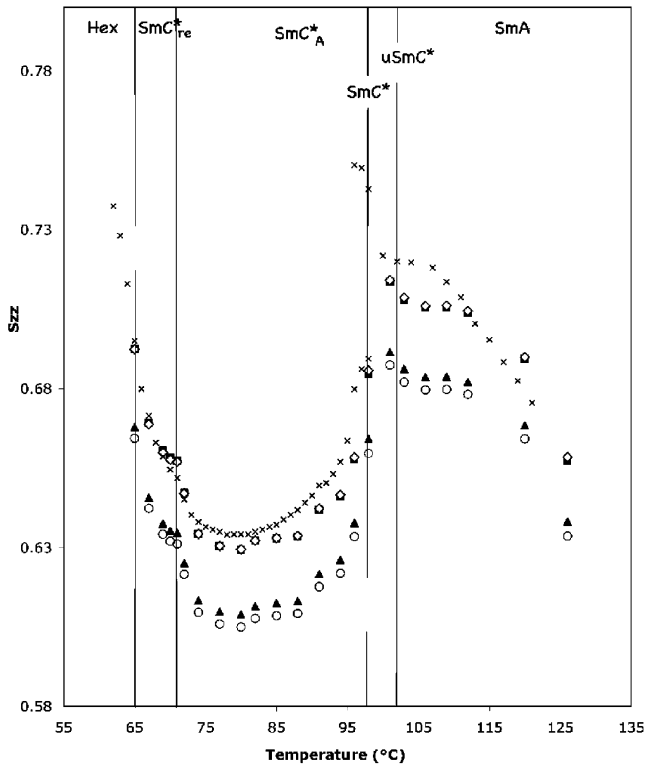

Figure 6. S_{zz} vs temperature trends as obtained from a previous ^2H NMR study[11] (crosses) and from ^{13}C chemical shifts as described in the text, using: (i) "regular" geometry and δ principal values from SUPER (open circles); (ii) DFT geometry and δ principal values from SUPER (full triangles); (iii) "regular" geometry and δ principal values from DFT (full squares); and (iv) DFT geometry and δ principal values from DFT (open rhombs).

5. Determination of Orientational Order Parameters

All the anisotropic chemical shifts measured from $^{13}C-^1H$ static spectra for the aromatic and carbonyl carbons were simultaneously analyzed using eqs 1 and 2 in purposely written software and exploiting nonlinear least-squares methods to give molecular orientational order parameters. To test the sensitivity and reliability of the orientational order parameters so obtained, we used in the calculations either experimental (SUPER) or theoretical (DFT) principal values of the shielding tensors, and either theoretical (DFT) or "regular" geometric parameters (i.e., orientation of the principal axes frame for the shielding tensor with respect to the molecular frame; see Table 1). The Saupe matrix has been assumed to be diagonal in a molecular frame in which the *z*-axis is coincident with the biphenyl para-axis, and the *x*-axis is in the ring plane (see Figure 2b). An angle α has been considered between the para-axes of the biphenyl and phenyl moieties and could be derived from the chemical shift analysis. Furthermore, it is known[26] that the phase biaxiality is negligible in the chiral tilted smectic phases (including the SmC^*_{re} phase of ZLL 7/*[27]), such that eq 1 has been used throughout all the studied LC phases here. The orientational order parameter results obtained for the different cases are reported in Figure 6, where they are also compared with those previously obtained from a ^2H NMR study.[10] In all of the cases, the isotropic chemical shift values δ_{iso} (MAS), determined by ^{13}C CP-MAS experiments recorded at relevant temperatures (see Supporting Information) within the LC phases, have been used in eq 3, rather than the isotropic values obtained from ^{13}C MAS experiments recorded in solution or in the solid state. Indeed, not only, as previously discussed (see Table 2), are detectable differences present among these sets of isotropic chemical shifts, but also a slight dependence on the temperature is exhibited by δ_{iso} (MAS), which might sensibly affect the orientational order parameters obtained.

As far as the orientation of the chemical shielding tensors is concerned, the "regular" geometry used in the calculations consisted in taking (i) for the tertiary aromatic carbons, the *z*-axis of the PAS frame along the aromatic C−H bond, considered to form an angle of either 60 or 120° with respect to the para-axis of the aromatic fragment; (ii) for the quaternary aromatic carbons, the *z*-axis along the para-axis; and (iii) for the carbonyl carbons, the *z*-axis along the C═O bond, considered to form an angle of 120° with respect to the para-axis of the closest aromatic fragment (see Table 1). In all of these cases, the *x*-axis is in the plane of the aromatic rings.

From Figure 6, it is evident that the choice of the orientations of the shielding tensors with respect to the molecular frame is not particularly critical: the use of the "regular" geometry gives orientational order parameters almost co-incident with those arising from the use of the "correct" geometry, as derived from DFT, reported in Table 1. On the contrary, despite their excellent agreement, already discussed, and shown in Table 1, the use of chemical shielding principal values from DFT calculations or SUPER experiments gives detectably different $\mathbf{S}_{zz}$ values, which result in being systematically larger by about 3% in the case of DFT. As it is possible to see from Figure 6, the $\mathbf{S}_{zz}$ trends obtained from the ^{13}C chemical shifts are in very good agreement with those previously derived from ^{2}H biphenyl quadrupolar and dipolar splittings,[10] despite that the two procedures are completely independent, the deuterium values being almost co-incident with those derived from ^{13}C DFT ones. In all the ^{13}C fitting cases, the molecular biaxiality ($\mathbf{S}_{xx}-\mathbf{S}_{yy}$) is very low throughout the mesophasic range investigated, being between 0.03 and 0.08 and between 0.07 and 0.11 using DFT and SUPER chemical shielding tensors, respectively, while it was imposed as null in the previous ^{2}H NMR study. A final consideration has to be made for the α angle between the para-axes of the two aromatic fragments, obtained from the fitting of the experimental data with the assumption that it does not change with temperature: its value ranges from 4.7 to 9.9° for the different fitting cases, while the value obtained from in vacuo DFT calculations is 8.5°, and a value close to zero was found from the previous ^{2}H NMR study.[10]

6. Conclusion

The present work represents an attempt to test the sensitivity in the choice of carbon shielding tensors, both their magnitudes and orientations, in the determination of molecular orientation ordering by analyzing ^{13}C anisotropic chemical shifts in the mesophases of a LC. In particular, DFT calculated and SUPER carbon shielding tensors were compared and found to essentially give identical principal tensorial components. This is gratifying despite the fact that different approaches were used. An added advantage of DFT calculations of carbon shielding tensors is the ability to locate the orientation of each tensor in a particular molecular frame. This information is indeed a necessary requirement to unambiguously find the orientation order parameters. It is indeed interesting to find that the "regular" geometry often assumed for the orientations of the shielding tensors is as good as those derived from the DFT method, as far as finding the ordering of the ZLL 7/* molecule is concerned. All our results based on the ^{13}C experiments in ZLL 7/* agree with those obtained by an independent ^{2}H NMR study. We have shown that the combination of experimental ^{13}C solid-state NMR techniques and ab initio DFT methods is a powerful and reliable methodology to derive molecular structure and orientational ordering information in bulk liquid−crystalline compounds. This is the second paper where this methodology is applied to chiral ferroelectric liquid crystals, after the work by Nakai et al.,[23] and the first one where molecular biaxiality has been taken into account in the evaluation of orientational order. Even though ^{13}C NMR represents a more complex route than ^{2}H NMR, this work suggests that the recent progresses in both theoretical and experimental techniques can allow the determination of reliable structural and ordering information. This not only overcomes the problem of synthesizing suitably deuterated compounds but might also allow the detailed study of molecular moieties (such as esteric groups) inaccessible to ^{2}H NMR.

Acknowledgment. The Natural Sciences and Engineering Council of Canada, and the Canada Foundation of Innovation and Italian MIUR (PRIN 2005 035119) are thanked for their financial support. J.Z. thanks Brandon University for financial support.

Supporting Information Available: Plots of δ_{iso} MAS (ppm) vs temperature (°C). This material is available free of charge via the Internet at http://pubs.acs.org.

References and Notes

(1) Dong, R. Y. Advances in NMR Studies of Liquid Crystals. In *Annual Report on NMR Spectroscopy*; Webb G., Ed.; Elsevier: Amsterdam, 2004; Vol. 53, Ch. 2.

(2) Geppi, M.; Veracini, C. A. Chiral Smectic Phases: NMR Studies. In *Encyclopedia of Nuclear Magnetic Resonance*; Grant, D. M., Harris R. K., Eds.; John Wiley: New York, 2002; Vol. 9, p 506.

(3) Liu, S. F.; Mao, J. D.; Schmidt-Rohr, K. *J. Magn. Reson., Ser. A* **2002**, *155*, 15.

(4) Kolbert, A. C.; Griffin, R. G. *Chem. Phys. Lett.* **1990**, *166*, 87.

(5) Hu, J. Z.; Orendt, A. M.; Alderman, D. W.; Pugmire, R. J.; Ye, C.; Grant, D. M. *Solid State Nucl. Magn. Reson.* **1994**, *3*, 181.

(6) Dong, R. Y.; Zhang, J.; Fodor-Csorba, K. *Chem. Phys. Lett.* **2006**, *417*, 475.

(7) Xu, J.; Fodor-Csorba, K.; Dong, R. Y. *J. Phys. Chem. A* **2005**, *109*, 1998.

(8) Kaupp, M.; Buhl, M.; Malkin, V. G. *Calculation of NMR and EPR Parameters*; Wiley VCH: Weinheim, Germany, 2004.

(9) Fung, B. M.; Khitrin, A. K.; Ermolaev, K. *J. Magn. Reson.* **2000**, *142*, 97.

(10) Catalano, D.; Domenici, V.; Marini, A.; Veracini, C. A.; Bubnov, A.; Glogarova, M. *J. Phys. Chem. B* **2006**, *110*, 16459.

(11) Kaspar, M.; Hamplova, V.; Novotna, V.; Glogarova, M.; Pociecha, D.; Vanek, P. *Liq. Cryst.* **2001**, *28*, 1203.

(12) Tycko, R.; Dabbagh, G.; Mirau, P. A. *J. Magn. Reson.* **1989**, *85*, 265.

(13) de Azevedo, E. R.; Hu, W. G.; Bonagamba, T. J.; Schmidt-Rohr, K. *J. Chem. Phys.* **2000**, *112*, 8988.

(14) Bennett, A. E.; Rienstra, C. M.; Auger, M.; Lakshmi, K. V.; Griffin, R. G. *J. Chem. Phys.* **1995**, *103*, 6951.

(15) States, D. J.; Haberkorn, R. A.; Ruben, D. J. *J. Magn. Reson.* **1982**, *48*, 286.

(16) Frisch, M. J.; Trucks, G. W.; Schlegel, H. B.; Scuseria, G. E.; Robb, M. A.; Cheeseman, J. R.; Montgomery, J. A., Jr.; Vreven, T.; Kudin, K. N.; Burant, J. C.; Millam, J. M.; Iyengar, S. S.; Tomasi, J.; Barone, V.; Mennucci, B.; Cossi, M.; Scalmani, G.; Rega, N.; Petersson, G. A.; Nakatsuji, H.; Hada, M.; Ehara, M.; Toyota, K.; Fukuda, R.; Hasegawa, J.; Ishida, M.; Nakajima, T.; Honda, Y.; Kitao, O.; Nakai, H.; Klene, M.; Li, X.; Knox, J. E.; Hratchian, H. P.; Cross, J. B.; Adamo, C.; Jaramillo, J.; Gomperts, R.; Stratmann, R. E.; Yazyev, O.; Austin, A. J.; Cammi, R.; Pomelli, C.; Ochterski, J. W.; Ayala, P. Y.; Morokuma, K.; Voth, G. A.; Salvador, P.; Dannenberg, J. J.; Zakrzewski, V. G.; Dapprich, S.; Daniels, A. D.; Strain, M. C.; Farkas, O.; Malick, D. K.; Rabuck, A. D.; Raghavachari, K.; Foresman, J. B.; Ortiz, J. V.; Cui, Q.; Baboul, A. G.; Clifford, S.; Cioslowski, J.; Stefanov, B. B.; Liu, G.; Liashenko, A.; Piskorz, P.; Komaromi, I.; Martin, R. L.; Fox, D. J.; Keith, T.; Al-Laham, M. A.; Peng, C. Y.; Nanayakkara, A.; Challacombe, M.; Gill, P. M. W.; Johnson, B.; Chen, W.; Wong, M. W.; Gonzalez, C.; Pople, J. A., Jr. *Gaussian 03*, revision B.05; Gaussian, Inc.: Pittsburgh, PA, 2003.

(17) Cheeseman, J. R. et al. *J. Chem. Phys.* **1996**, *104*, 5497.

(18) Ditchfield, R. *Mol. Phys.* **1974**, *27*, 789.

(19) Mason, J. *Multinuclear NMR*; Plenum Press: New York, 1987; Ch. 3.

(20) Eichele, K.; Wasylishen, R. *WSOLIDS1*, version 1.17.34; Dalhousie University: Halifax, Nova Scotia, 2001.

(21) Duncan, T. M. *Principal Components of Chemical Shift Tensors: A Compilation*; The Farragut Press: Madison, WI, 1997.

(22) Zheng, G.; Hu, J.; Zhang, X.; Shen, L.; Ye, C.; Webb, G. A. *J. Mol. Struct.* **1998**, *428*, 283−286.

(23) Nakai, T.; Fujimori, H.; Kuwahara, D.; Miyajima, S. *J. Phys. Chem. B* **1999**, *103*, 417.

(24) Blinc, R.; Dolinsek, J.; Luzar, M.; Seliger, J. *Liq. Cryst.* **1998**, *3*, 663.

(25) Fung, B. M.; Ermolaev, K.; Yu, Y. L. *J. Magn. Reson.* **1999**, *138*, 28.

(26) Xu, J.; Veracini, C. A.; Dong, R. Y. *Phys. Rev. E* **2005**, *72*, 51703.

(27) Veracini, C. A.; Domenici, V.; Marini, A.; Zhang, J.; Dong, R. Y. *ChemPhysChem*, submitted.